สำนักงานวิทยทรัพยากร จุฬาลงกรณ์มหาวิทยาลัย

CHAPTER IV
RESULTS AND DISCUSSION

4.1 Thermodynamic Equilibrium

Since corrosion reactions are reversible, the thermodynamics of equilibrium were studied to determine what specie is stable at the conditions of interest. For high temperature deaerated alkaline solution, it is generally known that the main corrosion product of water that reacts with iron is magnetite.

$$3Fe(s) + 4H_2O(g) \leftrightarrow Fe_3O_4(s) + 4H_2(g) \qquad (4.1)$$

The equilibrium constant (K) is a function of temperature. It can be calculated by using the value of the standard Gibbs free energy (G^0).

$$\Delta G^0 = -RT \ln K = \sum \nu_i \Delta G_i^f \qquad (4.2)$$

where ν_i is stoichiometric coefficient, and ΔG^f is Gibb free energy of formation.

The equilibrium constant is related to the partial pressure of the gases at equilibrium as shown in the following equation.

$$K = \frac{(P_{H_2})^4}{(P_{H_2O})^4} \qquad (4.3)$$

The effect of temperature on the equilibrium constant is determined through the Gibbs-Helmholtz equation (Perry *et al.*, 1984) as shown below.

$$\frac{d(\Delta G^0 / RT)}{dT} = \frac{-\Delta H^0}{RT^2} \qquad (4.4)$$

Where ΔH^0 is the standard heat of reaction and is the conventional symbol for $\sum(\nu_i H_i^0)$. Combination of Equations 4.2 and 4.4 gives,

$$d \ln K / dT = \Delta H^0 / RT^2 \qquad (4.5)$$

The dependence of ΔH^0 on temperature is given by

$$\frac{d(\Delta H^0)}{dT} = \Delta C_p^0 \qquad (4.6)$$

where $\Delta C_p^0 \equiv \sum(\nu_i C_i^0)$. Integration of Equation 4.6 requires that ΔC_p^0 be known as a function of temperature. Then

$$\Delta H^0 = \Delta H^f + \int \Delta C_p^0 dT \ . \qquad (4.7)$$

where ΔH^f is standard heat of formation.

By using Equations 4.3, 4.5 and 4.7, the temperature dependence of the equilibrium ratio of the partial pressures in the system can be calculated. The calculation is shown in Appendix A. A plot of the $(1/\sqrt[4]{K})$ vs T (°C) on semi-log scale will give a graph relationship between the ratios of water to hydrogen partial pressure (P_{H_2O}/P_{H_2}) versus temperature as shown in Figure 4.1.

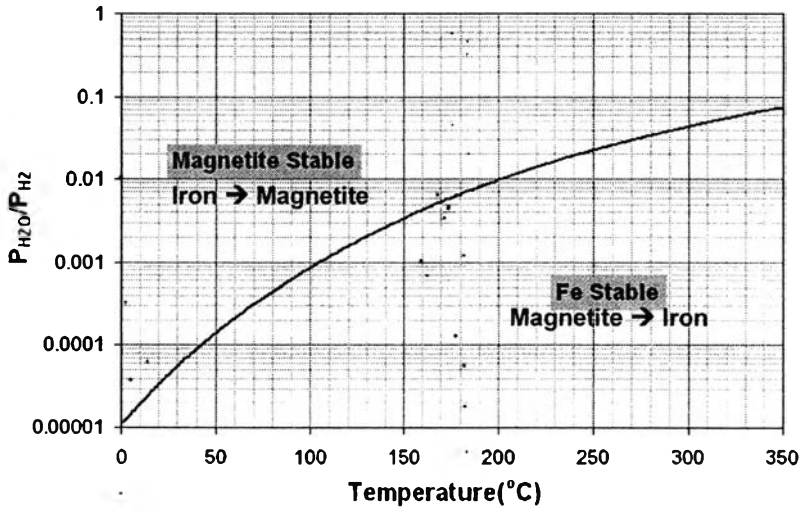

Figure 4.1 The graph relationship between ratio of hydrogen to water partial pressure (P_{H_2O}/P_{H_2}) and temperature.

From the equilibrium curve, it shows that the equilibrium ratio of water to hydrogen partial pressure is higher as the temperature increases. For any given temperature, magnetite is thermodynamically stable when the value of P_{H_2O}/P_{H_2} is above the line on Figure 4.1. On the other hand, when the value of P_{H_2O}/P_{H_2} is below the line, iron is thermodynamically stable. At an operating temperature of 300 °C, P_{H_2O}/P_{H_2} ratio is 0.043. Since water vapor pressure at 300 °C is 8766 kPa, partial pressure of hydrogen must be at least 203,864 kPa (8766 kPa / 0.043) in order to react with magnetite and form iron, which is very high. For a system that is operated at lower temperatures, the P_{H_2O}/P_{H_2} ratio is even lower. Thus it can be concluded that

4.2 Hydrogen Transport Through Solid

4.2.1 Mathematics of Hydrogen Diffusion

The process of hydrogen diffusion in and out of a metal resembles the process of heat transfer and both are descried by the same differential equations. The analogy of hydrogen diffusion to heat transfer may be applied for example; the diffusion of hydrogen is analogous to the flow of heat, and hydrogen diffusion coefficient is analogous to thermal diffusivity (A. A. Astaf'ev, 1991).

If one face, x = 0, of a membrane is kept at a constant concentration C_1 and the other, x = l, at C_2, and the membrane is initially at a uniform concentration C_0, there is a finite interval of time to reach the steady-state condition. During this time the concentration changes according to Equation 4.8 (J. Crank, 1956).

$$C = C_1 + (C_2 - C_1)\frac{x}{l} + \frac{2}{\pi}\sum_{n=1}^{\infty}\left[\frac{C_2\cos n\pi - C_1}{n}\sin\frac{n\pi x}{l}\exp\left(\frac{-Dn^2\pi^2 t}{l^2}\right)\right]$$

$$+\frac{4C_0}{\pi}\sum_{m=0}^{\infty}\frac{1}{(2m+1)}\sin\frac{(2m+1)\pi x}{l}\exp\left(\frac{-D(2m+1)^2\pi^2 t}{l^2}\right) \qquad (4.8)$$

For the commonest experimental arrangement, the membrane is initially at zero concentration, the concentration at the face which the diffusing substance emerges is maintained effectively at zero concentration and the opposite face is raised to C_2. Thus both C_0 and C_1 are zero. In this case Equation 4.8 reduces to;

$$\frac{C}{C_2} = \frac{x}{l} + \frac{2}{\pi}\sum_{n=1}^{\infty}\left[\frac{\cos n\pi}{n}\sin\frac{n\pi x}{l}\exp\left(\frac{-Dn^2\pi^2 t}{l^2}\right)\right] \qquad (4.9)$$

Graphs of C/C_2 are shown for various times in Figure 4.2 when Dt/l^2 and x/l are dimensionless parameters. Consequently, the solution for all values of D, l, t and x can be obtained from this graph. The steady state is achieved when Dt/l^2 equals approximately 0.45. The first substance permeates the sample when Dt/l^2 equals 0.0654 which is called the breakthrough time, t_b (Chalaftris, 2003). This relation can be used in practice to estimate the time required for hydrogen to diffuse through the pipe wall suddenly exposed to hydrogen. These values depend on the value of the diffusion coefficient of hydrogen in the steel. A higher diffusivity gives a lower time required for the hydrogen to reach the outside surface.

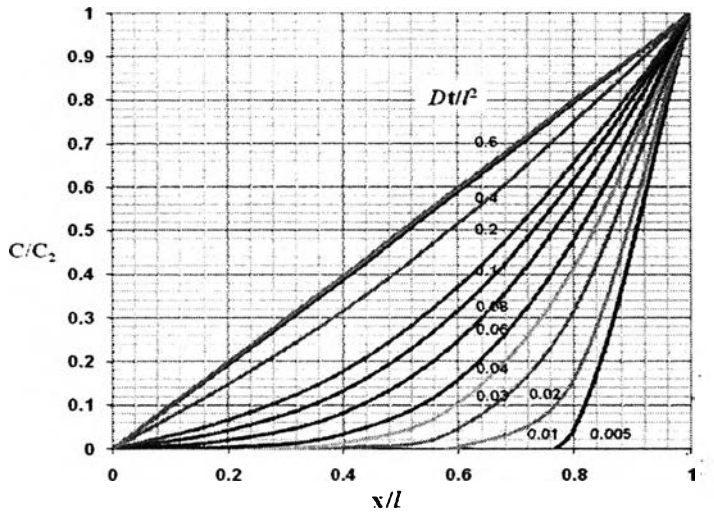

Figure 4.2 Concentration distributions at various times with initial uniform concentration C_0 and surface concentration C_2 at one side, zero at the opposite side. Numbers on the curves are values of Dt/l^2.

The total amount of diffusing substance, Q_t, which has passed through the membrane in time t, is shown in Equation 4.10.

$$\frac{Q_t}{lC_2} = \frac{Dt}{l^2} - \frac{1}{6} - \frac{2}{\pi^2}\sum_{n=1}^{\infty}\left[\frac{(-1)^n}{n^2}\exp\left(\frac{-Dn^2\pi^2 t}{l^2}\right)\right] \tag{4.10}$$

As $t \to \infty$, this becomes,

$$Q_t = \frac{DC_2}{l}\left(t - \frac{l^2}{6D}\right) \tag{4.11}$$

Which is a straight line with an intercept, L, on the t axis given by,

$$L = \frac{l^2}{6D} \tag{4.12}$$

Equation 4.12 provides an easy means of measuring the diffusivity of hydrogen and is called the time lag method. Equation 4.10 is plotted as a function of Dt/l^2 as shown in Figure 4.3.

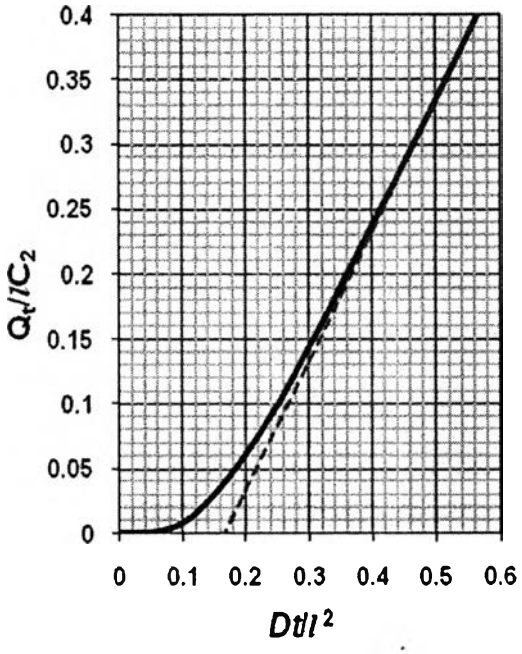

Figure 4.3 Approach to steady-state flow through an infinite plate of thickness L.

If the initial concentration in the plate is C_0, and at the ingoing and outgoing surfaces, C_1 and C_2 respectively, the asymptote cuts the time axis at the point,

$$L = \frac{d^2}{6D}\frac{1}{(C_1 - C_2)}\left[\frac{C_2}{6} + \frac{C_1}{3} - \frac{C_0}{2}\right]. \qquad (4.13)$$

This method is applicable to gas flow through metals. Plotting the pressure in the high-vacuum side against time tends to the steady state asymptotically. Thus the expression $L = \frac{d^2}{6D}$ gives a value of the diffusion coefficient.

This formula is applicable only if

1) Interface reactions are fast compared with the diffusion process. Since this equation does not take account of the time lag associated with the transition of hydrogen atoms from the adsorbed to the adsorbed state.

2) The concentration of the diffusing substance at the external boundary is reached instantaneously and remains constant for the duration of the process

3) The concentration of the diffusing substance at the internal boundary is substantially lower than that at the external boundary.

4) The material is very thick or the diffusion coefficient of media is very small. The values of D determined by this method are underestimated when it is applied to thin specimens since the specimen thickness affects D. However, D becomes independent of specimen thickness when the specimen is large.

The other way for calculating the diffusivity is by using breakthrough time (t_b) or the time that hydrogen first permeates through the membrane,

$$t_b = \frac{l^2}{15.3D} \tag{4.14}$$

These methods can be applied to the diffusion of gases through hot metals, or to the diffusion of nascent gases liberated at room temperatures by electrolysis or by chemical reaction at the metal surface (R.M. Barrer, 1951).

4.2.2 The Breakthrough Time of Hydrogen Diffusion

By using the breakthrough time method ($Dt/l^2 = 0.0654$), the time required for hydrogen to diffuse through a steel pipe wall can be estimated. For the calculation, the diffusion coefficient of hydrogen is required. However, the hydrogen diffusivity of the same types of carbon steel as used in the experiments and the field have not been determined. Thus an average value of hydrogen diffusivity through iron obtained from the literature was used in calculations presented in Appendix D.

It is generally accepted that the hydrogen diffusivity of carbon steel is lower than that of pure iron. Addition of alloy elements reduces the diffusivity. Thus the hydrogen diffusivity used in this calculation is one order of magnitude lower than the hydrogen diffusivity in pure iron at the temperature of interest.

For the experiment in Loop 1, the process was started at 80°C and the thickness of the tube wall was 2.18 mm. The hydrogen diffusivity is assumed to be 8×10^{-10} m^2/s since the hydrogen diffusivity of iron at 80°C is 8×10^{-9} m^2/s. Therefore the estimate of time for hydrogen to first appear through the tube wall is 6.48 minutes. In the case of the HEP on the feeder pipe at PLGS, the process was started at 310°C and the thickness of the pipe wall is 6 mm. The hydrogen diffusivity is as-

sumed to be 2.2×10^{-9} m^2/s since the hydrogen diffusivity of iron at 80°C is 2.2×10^{-8} m^2/s. Thus the estimated time for hydrogen to first appear through the feeder pipe wall at PLGS is 17.6 minutes.

4.2.3 Estimation of Hydrogen Diffusivity by the Time Lag Method

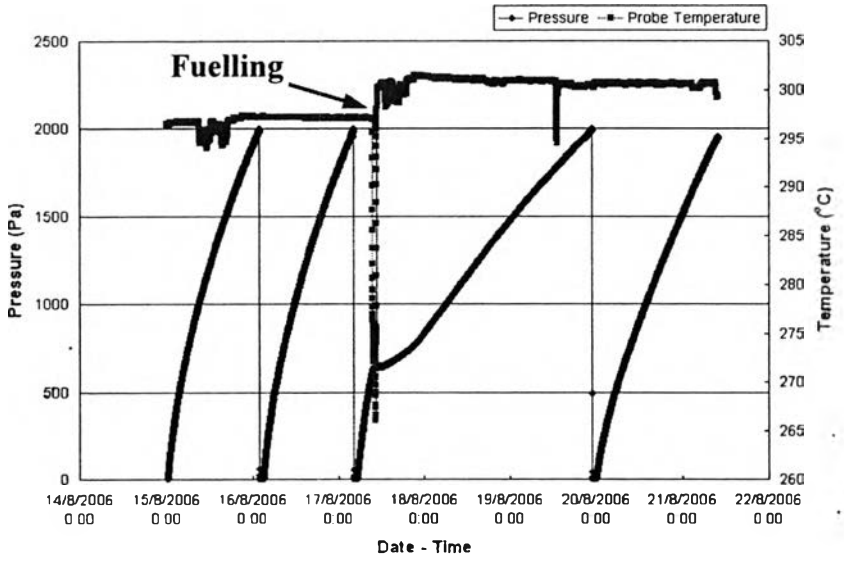

Figure 4.4 Pressure measurement at PLGS during August 2006.

A HEP was installed on an outlet feeder pipe of a CANDU reactor at the Point Lepreau Generating Station (PLGS) during the 2006 station maintenance outage (McKeen *et. al*, 2007). The HEP has been used to monitor the corrosion of the carbon steel feeder pipe. Data of the hydrogen pressure measurement from August 14th to 22nd is shown in Figure 4.4. On August 17th, the hydrogen pressure increase was interrupted by the station fuelling the channel corresponding to the HEP. During fuelling, the coolant system is exposed to significant concentrations of dissolved oxygen. The pressure stopped rising after the fuelling as shown in Figure 4.5. This indicates that the production of atomic hydrogen from FAC on the inner surface of the pipe had ceased, presumably because the reduction of hydrogen ions is replaced by the reduction of oxygen. Thus, there is no increase in HEP pressure while

there is a presence of oxygen in the fluid (Scott *et al.*, 2007). However, the HEP pressure started to increase again after all the oxygen was consumed.

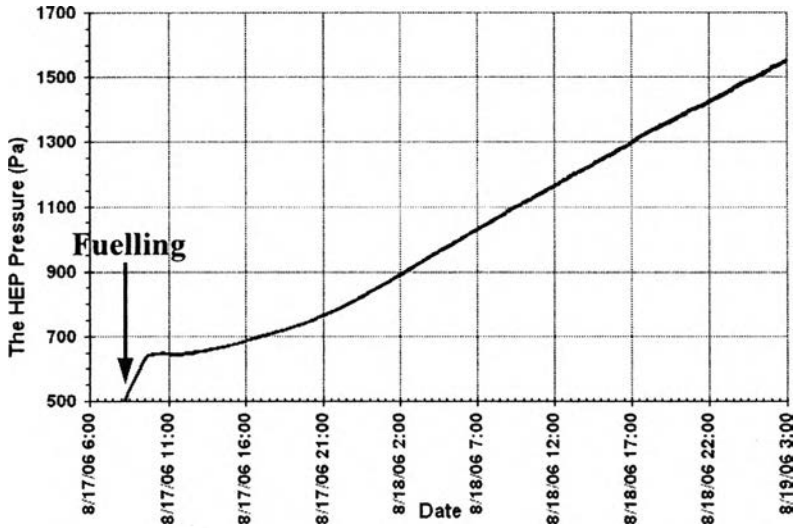

Figure 4.5 The HEP pressure change during the fuelling on August 17th.

From Figure 4.5, the diffusion coefficient can be estimated immediately after the fuelling, using the Time-Lag Method. The calculation procedure is shown in Appendix B. From the calculation, the diffusion coefficient of hydrogen through the carbon steel pipe at PLGS was determined to be 2.38×10^{-10} m^2/s when the operating temperature is 310 °C. The diffusion coefficient from this calculation is one order of magnitude lower than the values from the literature which were reported to be in the range of $2\text{-}3\times10^{-9}$ m^2/s at 310 °C. It is expected that the oxide film at the metal surface reacted with oxygen and changed its form. After all the oxygen was consumed, the oxide film was then converted back to the steady-state form in deaerated solution. Transformation of the oxide film results in changing the corrosion rate which extended the time to approach steady state. It can be seen that the corrosion rate after adding oxygen is lower than the corrosion rate before adding oxygen.

The time lag method takes account of the time that hydrogen starts to diffuse at a constant corrosion rate until steady state diffusion is reached. However, when adding oxygen to the solution, the residence time included the time taken for the corrosion reaction to consume all the oxygen, the time to change the oxide film

back to its steady form, and the time for the corrosion rate to return to a constant rate. Thus the time lag from this calculation is overestimated and results in a lower hydrogen diffusivity.

4.3 Hydrogen Monitoring at the Coleson Cove Generating Station

An HEP was installed on a water-wall tube of Boiler #1 at the Coleson Cove Generating Station during the 2007 maintenance outage. The effects of changes in pH of the boiler feed-water and the load of the boiler were measured. The data collected during October 1st to December 19th, 2007 were collected as shown in Figure 4.6 and 4.7. The bar chart in Figure 4.8 and 4.9 show the effect of the boiler load and the pH of the solution on the rate of pressure rise (Pa/day), respectively. The difficulty in analysing the data from Coleson Cove was that none of the operating parameters were constant.

Since the operating temperature was not constant, the reading of the HEP pressure was influenced by temperature changes. In order to eliminate the effect of temperature, the HEP pressure was adjusted by correcting the reading to account for temperature variations giving an effective temperature of 350 K. The adjusted pressure is plotted on the graphs and compared with the measured pressure.

4.3.1 Effect of the Load of the boiler

Figure 4.6 and 4.8 indicate that the rate of HEP pressure rise increases with load of operation. As the load increases, the flow rate and temperature of the solution normally increase which leads to an increasing corrosion rate and hence an increase in hydrogen generation as shown from Oct 6th to 11th. The data show, however, contradictions in some periods. Although the boiler was operated from Nov 10th to 20th, there was no indication of an increase in the HEP pressure. It can be noticed that the average load was less than 100 MW during this period. This could potentially be due to the load being too low in some periods for the hydrogen produced from corrosion to be accurately measured by the HEP. During Dec 2nd to 7th, the HEP pressure slightly increased when there was a high load but the HEP pressure did not increase after Dec 8th.

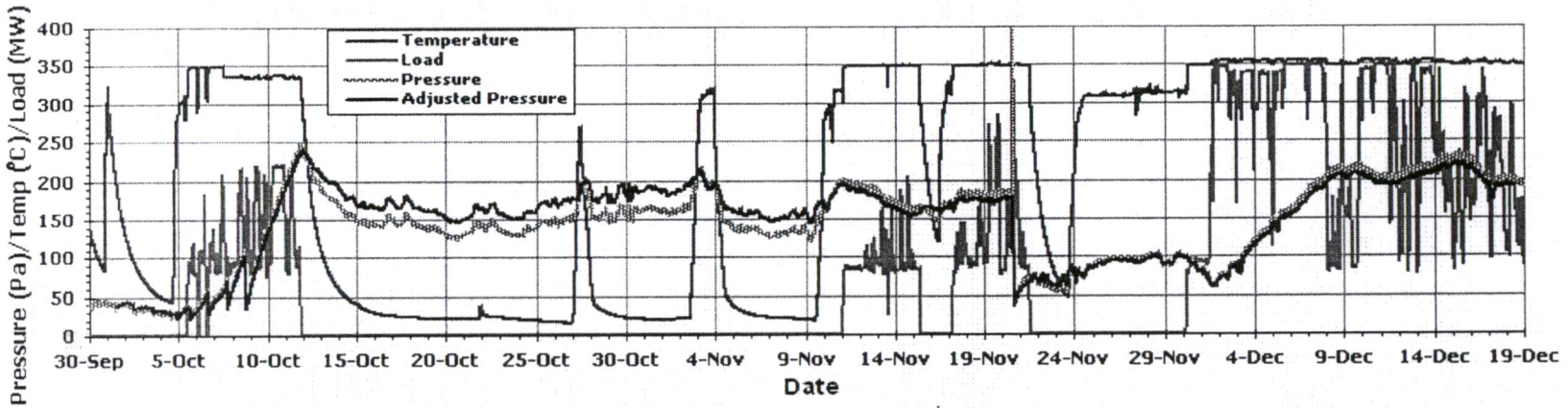

Figure 4.6 The plot of HEP pressure, boiler load and operating temperature vs. time from Coleson Cove.

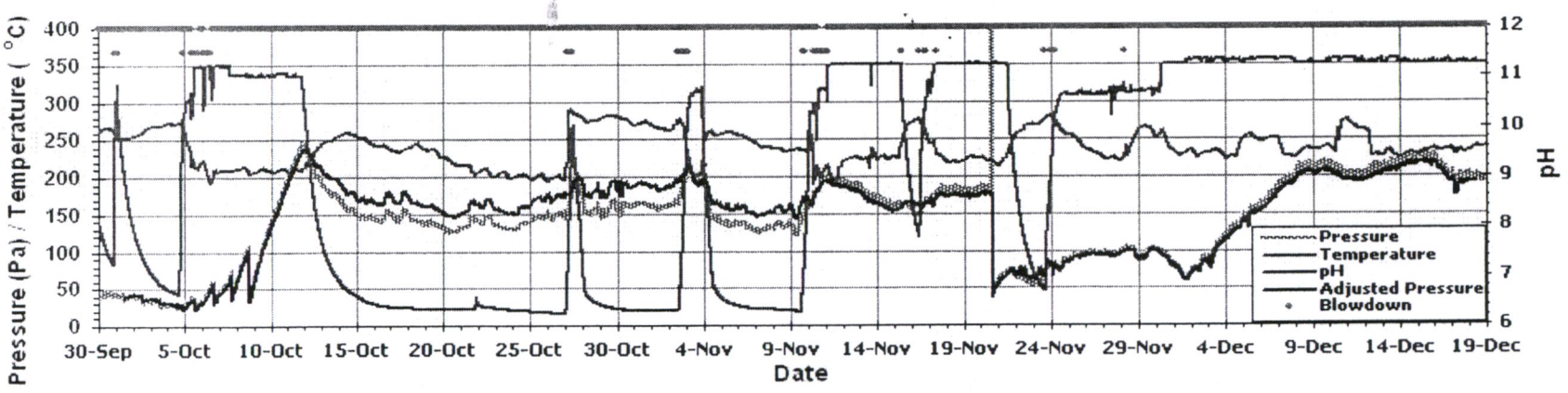

Figure 4.7 The plot of HEP pressure, pH of the solution, boiler blowdown and operating temperature vs. time from Coleson Cove.

It should be noted that on Nov 20th, the HEP pressure decreased because the system was pumped down. Figure 4.8 shows that when there was no load, the HEP pressure changed in the range of ±10 Pa/day due to the precision of the pressure transducer. Nevertheless, the HEP pressure changed up to ±25 Pa/day when there was a change in temperature despite no load. It is possible that a change in operating temperature affects the hydrogen formation from FAC, and hydrogen transport through the steel.

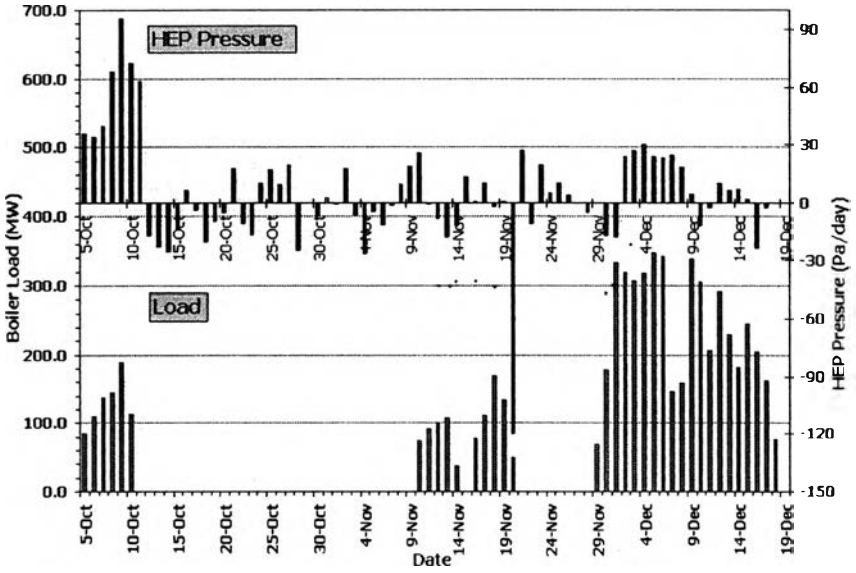

Figure 4.8 The HEP pressure accumulation (Pa/day) vs. the boiler load (MW).

4.3.2 Effect of the pH of the solution

The pH of the solution decreases when the temperature increases as shown in Figure 4.7. It can be estimated from the data that the normal operating pH is 9.5. However, the pH of the solution from Oct 6th to 11th was lower i.e. pH of 9.2.

From the graph, there are a few points where the pH changed while the temperature was constant. It seems that there was a loss of the HEP pressure when the pH increased i.e. Nov 29th, Dec 11th. It can be noticed that whenever pH was steady, the HEP pressure increased when there was a high load. On the other hand, the HEP pressure did not increase when the pH of the solution was unstable.

Considering the period that hydrogen obviously increased i.e. Oct. 6^{th} to 11^{th}, the pH of the solution was lower than during other periods as shown in Figure 4.9.

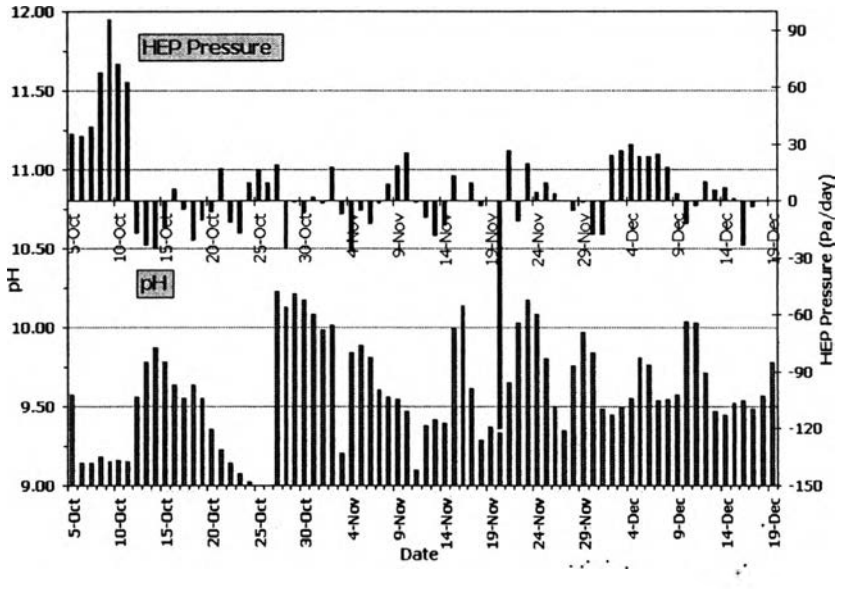

Figure 4.9 The HEP pressure accumulation (Pa/day) vs. pH of the solution.

It is believed that the corrosion rate of the boiler depends on the pH of the solution. The results show that the corrosion rate was higher at a lower pH. Thus hydrogen pressure increased when the pH of the solution was low. On the other hand, the corrosion rate may be too low to be measured by the HEP since the pH of the solution was higher during other periods. It should be noted that the pH of the solution was low during the last week of October, however, there was no increase in hydrogen pressure because there was no load during this period.

4.3.3 Boiler blowdown (Opened/Closed)

The blowdown status is shown in Figure 4.6. It is noted that a lower dot in the plot means the blowdown was opened and a higher dot means the blowdown was closed. The boiler blowdown was opened just before the process temperature was increased to the operating temperature. The effect of boiler blowdown on the HEP pressure cannot be determined from this data since other parameters i.e. pH and temperature also changed at the same time as the blowdown. However, it is ex-

pected that the chemistry of the solution was changed after the boiler blowdown and this change affected either the hydrogen transport or the corrosion rate.

In conclusion, the HEP pressure rate of increase changes with the operating load. The pH of the solution also influenced the HEP pressure rise. It is believed that the pH of the solution affects either the rate of corrosion or the hydrogen production. When the pH was increased, the data showed no increase in hydrogen pressure despite the high load.

4.4 Hydrogen Transport Through the Pressure Transducer Diaphragm

In addition to the study of the effects of operating parameters on the FAC-generated hydrogen, data from Coleson Cove showed that the accumulated hydrogen pressure was reduced when the process was not operated and there was no hydrogen removal. This indicated that some hydrogen was released from the HEP. Leaking from the HEP is not the reason of pressure reduction since the pressure inside the HEP is low compare to atmospheric pressure. If there was any leak, the air from outside would ingress into the HEP. The pressure transducer would thus show an increase in pressure.

The possible reasons for the pressure reduction are the escape of the hydrogen gas into the vacuum system, diffusion through the pressure transducer diaphragm made of Inconel, and diffusion of hydrogen back into the steel boiler tube. In this work, the amount of hydrogen that possibly diffuses through the diaphragm of the pressure transducer was determined.

The thin diaphragm which is made of Inconel divides the pressure side and the full-vacuum side within the probe. When pressure is applied to the diaphragm, its deflection produces a change in the distance between the electrodes and the diaphragm and results in a change of the capacitance as shown in Figure 4.10.

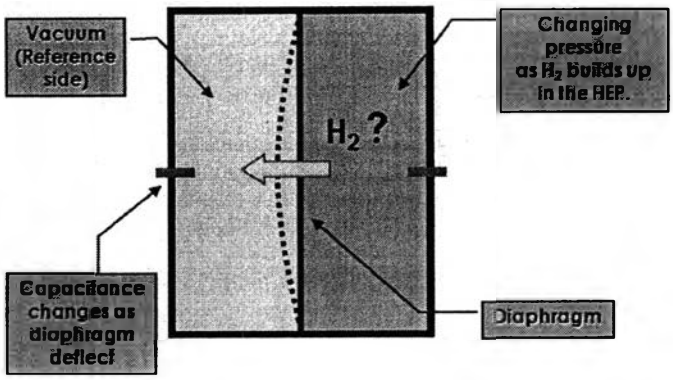

Figure 4.10 The chambers and the diaphragm inside the pressure transducer.

Hydrogen transport through the membrane can be described by "flux", which is defined as the rate of hydrogen passing through the membrane per unit area. The hydrogen flux can be calculated from Fick's First Law as shown below.

$$J = D\frac{(c_1 - c_2)}{l}, \tag{4.15}$$

where J is the diffusion flux, D is the diffusion coefficient of hydrogen through Inconel, c is the hydrogen concentration at $x = 0$ and $x = l$, and l *is* thickness of the diaphragm (2 mils or 5.08×10^{-5} m).

Another method is using the permeability equation as shown below,

$$J = \frac{k(P_{H_2(1)}^{0.5} - P_{H_2(2)}^{0.5})}{l} \tag{4.16}$$

where k is the hydrogen permeability of the membrane which in this case is the diaphragm, and P_{H_2} is partial pressure of hydrogen.

One side of the diaphragm is a full-vacuum ($C_2 = 0$), while the pressure on the other side depends on the amount of hydrogen that is produced from corrosion. In normal operation, the pressure within this side is pumped down when 2000 Pa is achieved. Hence, a pressure of 2000 Pa was used in this calculation.

The hydrogen diffusion coefficient (D) and the hydrogen permeability (ϕ) in Inconel from the literature are shown below,

W.M. Robertson (1977):

$$D_{Inconel\ 718} = 1.07 \times 10^{-6} \exp\left(\frac{-5992.2}{T}\right) \text{ m}^2/\text{s}. \quad (4.17)$$

$$\phi_{Inconel\ 718} = 8.09 \times 10^{-3} \exp\left(\frac{-6712.3}{T}\right) \text{ cm}^3(\text{NTP})/\text{cm}\cdot\text{s}\cdot\text{atm}^{1/2} \quad (4.18)$$

S.D. Felicelli *et al.*(2000):

$$D_{Inconel\ 718} = 1.2 \times 10^{-6} \exp\left(\frac{-6076}{T}\right) \text{ m}^2/\text{s} \quad (4.19)$$

J.Xu *et al.* (1994):

$$D_{Inconel\ 718} = 4.06 \times 10^{-7} \exp\left(\frac{-5849}{T}\right) \text{ m}^2/\text{s} \quad (4.20)$$

The diffusivities from the above equations give nearly the same value. The difference is less than one order of magnitude at the temperature of interest. The highest value of the hydrogen diffusivity which is reported by W.M. Robertson was used in this calculation.

The pressure transducer is operated at 45 °C. At this temperature, the hydrogen diffusivity and the hydrogen permeability of Inconel are 7.016×10^{-15} m^2/s and 5.562×10^{-12} $cm^3(NTP)/cm\cdot s\cdot atm^{1/2}$, respectively. (Note: 4.208×10^{-15} m^2/s from S.D. Felicelli, and 6.04×10^{-15} m^2/s from J.Xu)

The volume of the gas chamber inside the pressure transducer is 2.2 cm^3. If this chamber is rectangular in shape and one side of this chamber is the diaphragm, the volume is equal to the area of the diaphragm times the distance between the diaphragm and the wall. It is assumed that the distance between the diaphragm and the wall is 1 cm. Hence the area of the diaphragm is assumed to be 2.2 cm^2.

The calculation is shown in Appendix C. The results from this calculation show that the rate of hydrogen escaping through the pressure transducer diaphragm is extremely low. If the hydrogen produced from corrosion is 2000 Pa/day, only 0.34-0.54 Pa/day or 0.017-0.027% of hydrogen will be lost from diffusion through the pressure transducer diaphragm.

In addition, the sensitivity of each parameter was analyzed as shown in Figure 4.11 - 4.12. The hydrogen pressure that is collected inside the pressure transducer and the area of the diaphragm are directly proportion to the rate of hydrogen diffus-

ing through the diaphragm. On the other hand, the thickness of the diaphragm is inversely proportional to the hydrogen diffusion rate. The total volume of the HEP affects the change in pressure inversely.

It should be mentioned that the type of Inconel which was used to make the diaphragm is unknown. Since the hydrogen diffusivity and permeability depend on the type and properties of the material. In the calculation, the values of hydrogen diffusivity and permeability for Inconel 718 were used. Nevertheless, the value of hydrogen diffusivity and permeability are not expected to be much different.

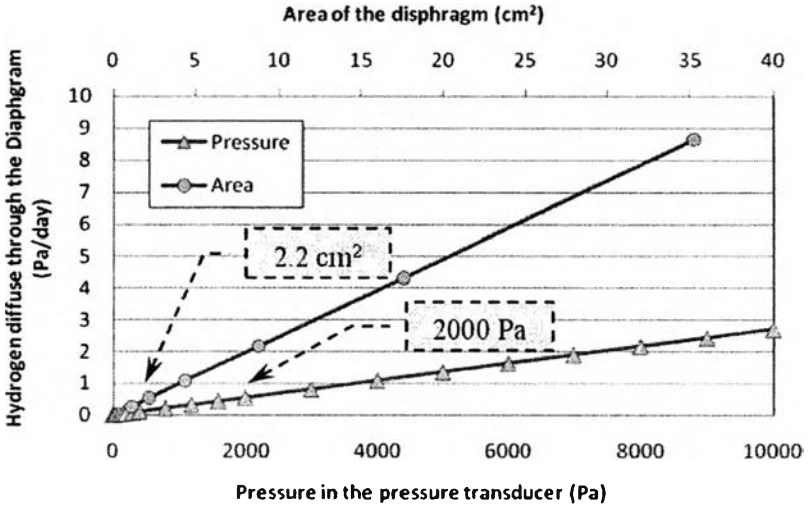

Figure 4.11 The possibility of hydrogen diffusion through the diaphragm when changing the area of the diaphragm and the highest pressure inside the HEP.

Calculations show the amount of hydrogen diffusion through the Inconel diaphragm should be negligible (less than 0.03%). Although the hydrogen diffusivity is a few orders of magnitude higher than the value that was used in this calculation, the loss of hydrogen via the diaphragm is still small. It indicates that hydrogen diffusion through the pressure transducer diaphragm is not the reason for losing hydrogen pressure in the HEP. It is expected that the hydrogen may be lost via the valve that connects the pressure transducer and the vacuum pump or via diffusion back into the carbon steel boiler tube. The hydrogen permeation experiment (Appendix F) shows that it is possible for hydrogen gas to dissociate and diffuse through the carbon steel

at high temperature. Unfortunately, there is no proof to indicate which of these hypotheses is more likely for hydrogen loss. Further investigation is required.

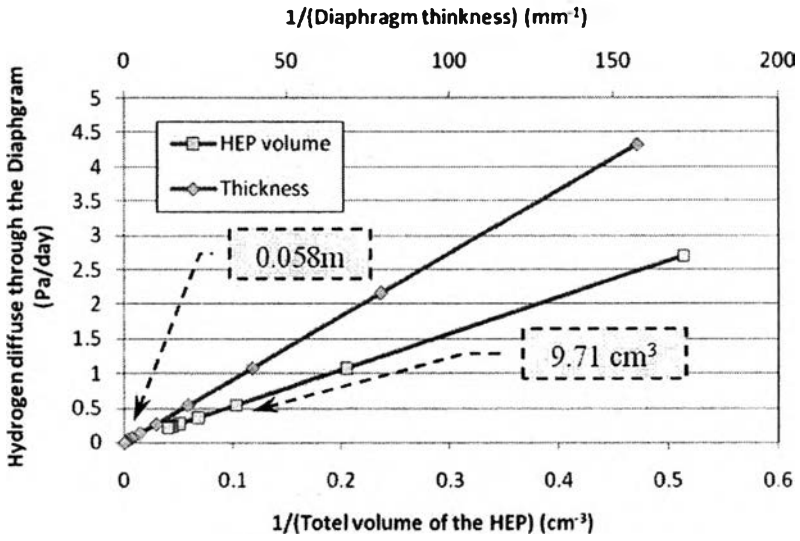

Figure 4.12 The possibility of hydrogen diffusion through the diaphragm when changing the diaphragm thickness and the total volume of the HEP.

4.5 Prediction of Hydrogen Permeation and Accumulation

The behavior of hydrogen transport was theoretically studied in order to predict the curve of hydrogen pressure rise by using Fick's Law (Barrer, 1951 and Crank, 1964). The configuration of the HEP and the thickness of carbon steel pipe from PLGS and Loop 1 were used in this calculation. In the case of the HEP installed at PLGS, cartesian coordinates were applied since a silver cup covered only a small part of the pipe. The cylindrical coordinates were applied in the case of the HEP in Loop 1 since the tube is surrounded by a silver annulus. The trend of hydrogen pressure increase from permeation through steel of PLGS and Loop 1 are shown in Figure 4.13 and 4.14, respectively.

These graphs represent systems with constant corrosion rates. Thus hydrogen produced from FAC at the metal/oxide interface was assumed to be constant. The pressure in the HEP increases as the hydrogen produced from the corrosion diffuses through the steel.

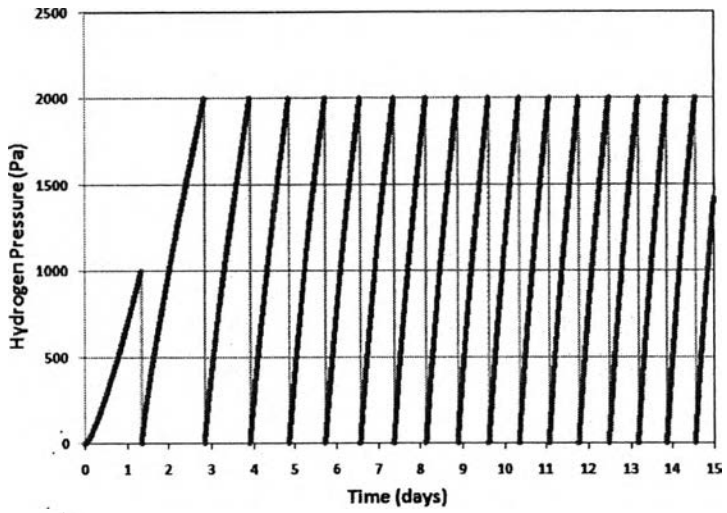

Figure 4.13 The prediction of hydrogen pressure in the HEP on the pressure accumulation using PLGS parameters (cartesian coordinates).

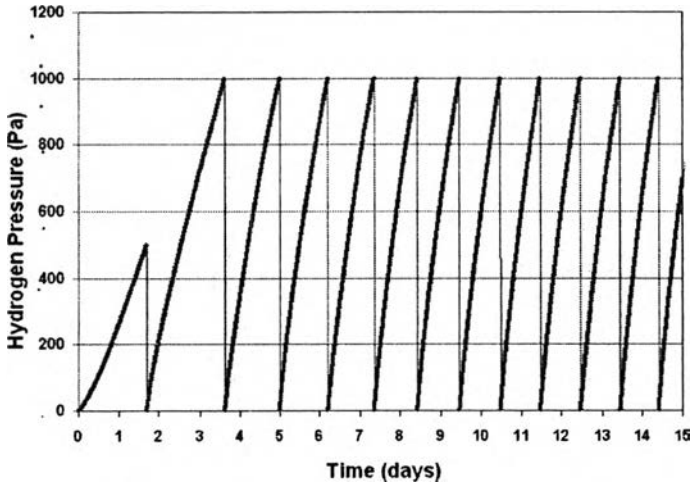

Figure 4.14 The prediction of hydrogen pressure in the HEP on the pressure accumulation using Loop 1 parameters (cylindrical coordinates).

It can be seen from the graphs that although the rate of hydrogen production is constant due to a constant corrosion rate, it takes a few days before hydrogen reaches steady state diffusion. Nevertheless, the corrosion rate is not constant, but it is normally high when starting a process since there is no passive film on a metal surface. In addition, without the oxide film, the FAC-produced hydrogen could go into

the solution instead of being absorbed into the metal. Thus, it is expected that the hydrogen pressure rise might not follow this trend on the first few days after a start-up.

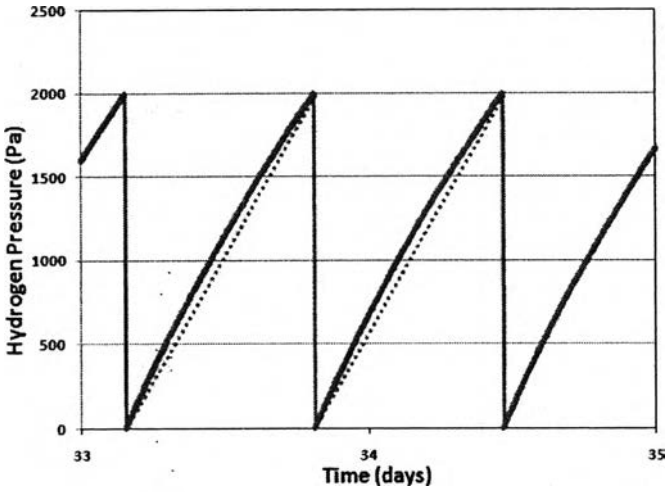

Figure 4.15 The prediction of curving behaviour of the pressure rise using PLGS.

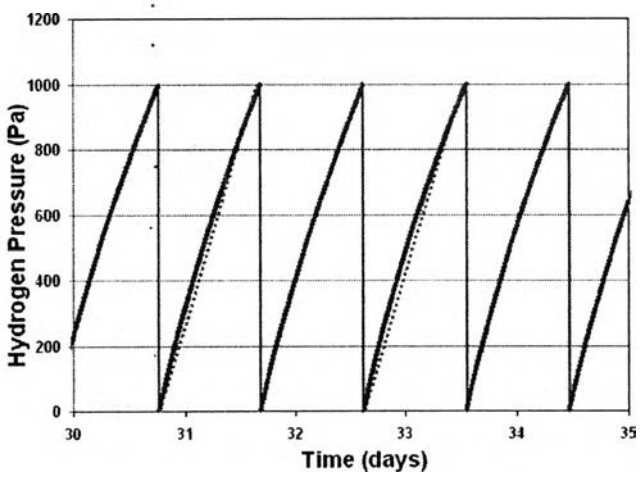

Figure 4.16 The prediction of curving behaviour of the pressure rise (Loop 1).

Figures 4.15 and 4.16 show the curving behavior of the pressure compared to straight dashed lines which represent constant corrosion with a constant diffusion rate. The reason for this curving is a decrease in the hydrogen diffusion rate due to an increase in pressure at the exit surface. The rate of hydrogen diffusion is higher when the accumulated HEP pressure is low as represented by a higher slope of the hydro-

gen pressure. After adjusting the HEP pressure to full-vacuum, the hydrogen can diffuse through the steel with a higher rate. Then the diffusion rate decreases as the HEP pressure increases. Thus the rate of pressure rise is a function of the pressure inside the HEP.

The appearance of curving depends on many factors such as the rate of hydrogen generation, the hydrogen diffusivity in the steel, the thickness of the pipe wall, the highest pressure in the HEP and the HEP configuration.

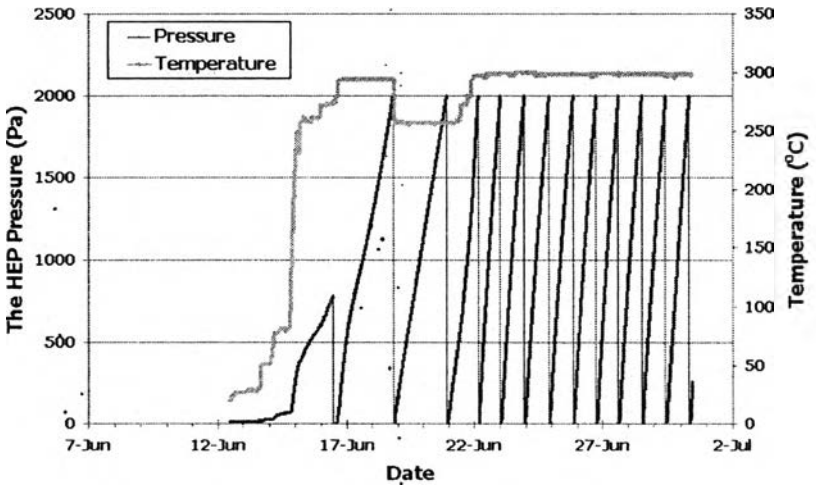

Figure 4.17 The plot of the HEP pressure from PLGS (McKeen *et al.*, 2007).

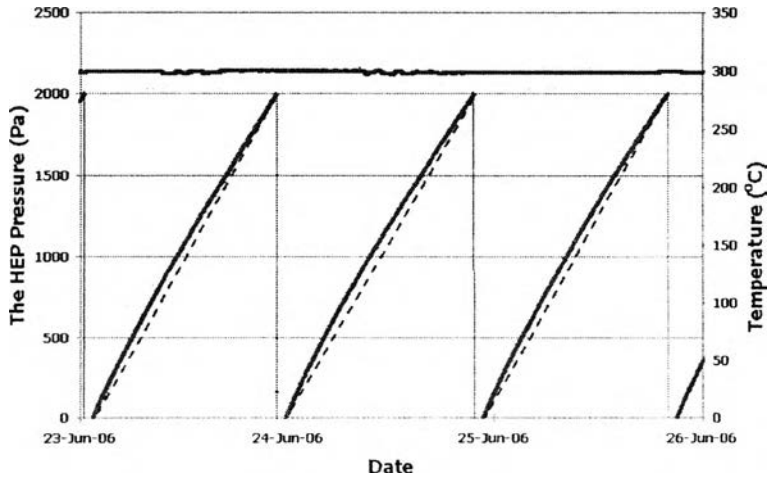

Figure 4.18 Non-linearity of hydrogen pressure from PLGS.

An HEP has been installed on an outlet feeder pipe at PLGS since June, 2006. The results of the measured HEP pressure during the first month of operation are shown in Figure 4.17. It can be noticed from Figure 4.18 that the pressure rise was non-linear. The behavior of curving shows the same trend as the predicted pressure based on hydrogen back pressure. Thus changing of the hydrogen diffusion rate may be the reason for non-linearity of the pressure curve.

However, the experiment in Loop 1 shows a different trend of the pressure rise. The results from Loop 1 reveal a linearity of the pressure rise as shown in Figure 4.19. Pressure up to 4000 Pa can be reached without affecting the pressure inside the HEP when steady state corrosion is reached.

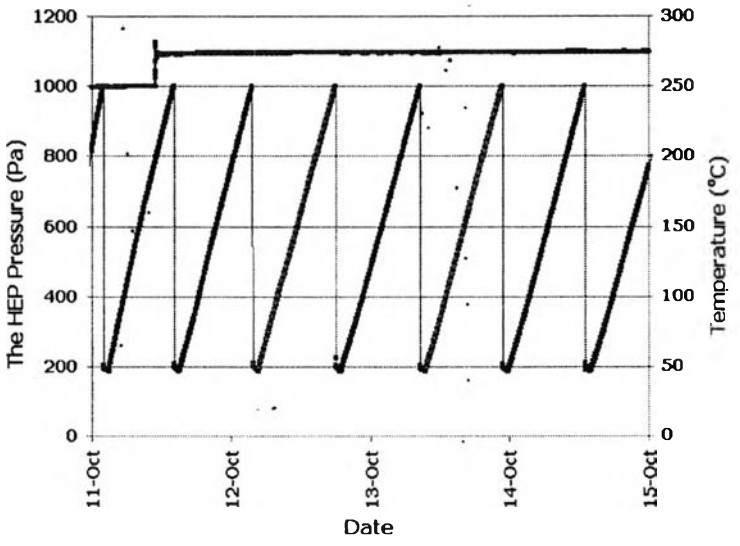

Figure 4.19 Non-linearity of hydrogen pressure from Loop 1.

If the accumulated pressure inside the HEP is not the reason for the curving of the HEP pressure rise from PLGS, the cause for this behavior may be imperfect sealing of the pressure transducer or the vacuum valve. It should be noted that the vacuum pump at PLGS maintains a vacuum at all times of operation. If there is any leak inside the HEP system i.e. at the vacuum valve, the pressure transducer will lose pressure. A higher pressure inside the HEP would lead to a greater pressure loss by

leaking into the vacuum. Thus the rate of pressure rise decreased as the HEP pressure increased.

Unlike the vacuum pump at PLGS, the vacuum pump in Loop 1 is operated only before a pump-down. Thus any leak inside the HEP system in Loop 1 will lead to an increase of the pressure caused by the atmospheric pressure which is about 10,000 times higher than the highest pressure inside the HEP.

4.6 The HEP Experiment in Loop 1

In the experiment in Loop 1 at CNER during Oct. 2006, the HEP was not degassed before starting the experiment. The results in Figure 4.20 showed that the rate of pressure rise was initially high in the first few hours after the valve in the test section was opened. This rise of pressure did not represent hydrogen gas but resulted from liberation of other gases that were contained inside the metal. Thus the purpose of out-gassing is to eliminate the presence of other gases in the HEP which leads to a higher measurement of hydrogen pressure rise.

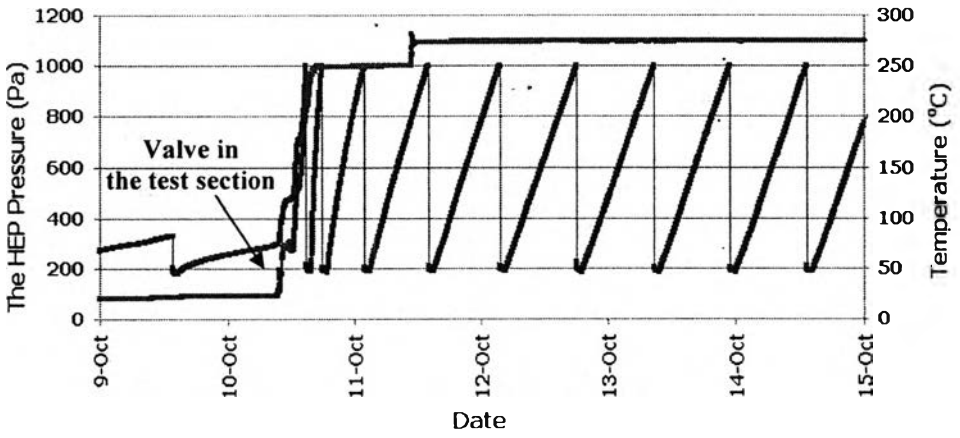

Figure 4.20 The plot of HEP pressure from the experiment on Loop 1 during Oct., 9th and Oct., 15th 2007.

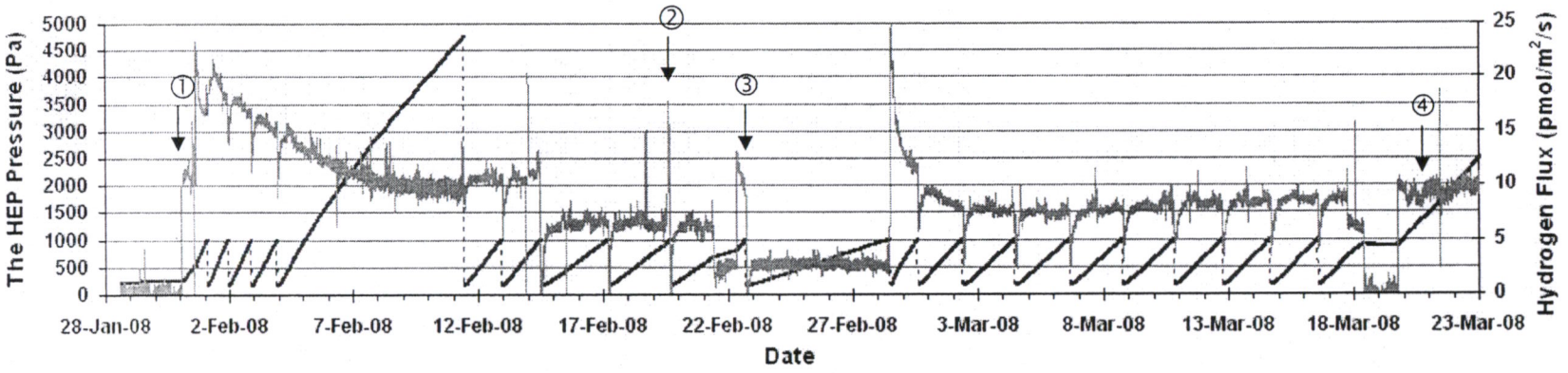

Figure 4.21 The plot of the HEP pressure and hydrogen flux vs. time from Loop 1.

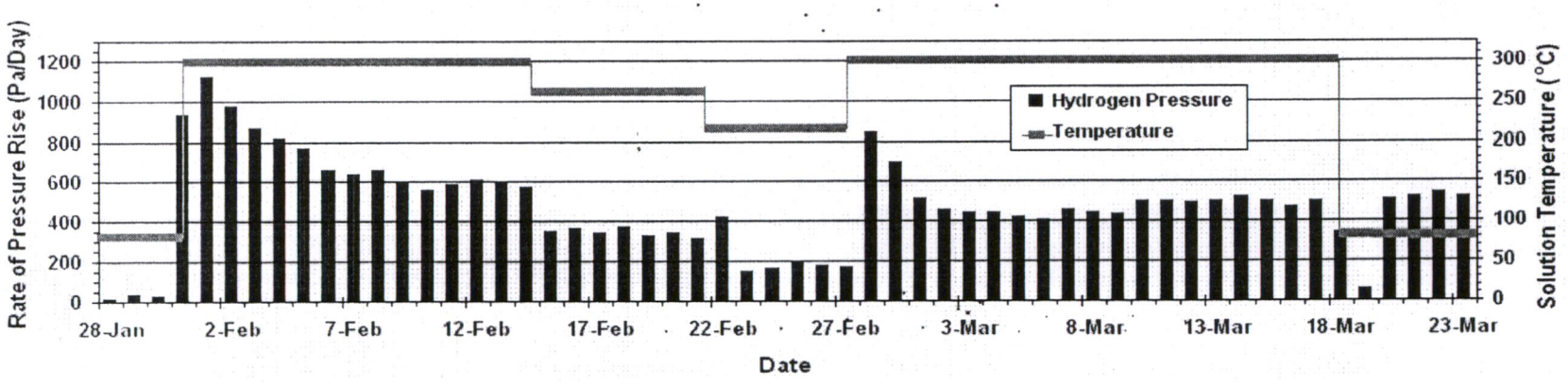

Figure 4.22 The plot of the rate of pressure rise and the solution temperature vs. time from Loop 1.

In this experiment, the HEP was degassed at 300°C until there was no HEP pressure increase which indicates that there was no gas inside the metal. Then Argon was purged into the test section prior to starting the experiment by valving-in the test section. The leak rate of the HEP was noted to be very low since the HEP pressure increase was less than 25 pa/day. The overall results from Jan., 28th to Mar., 23rd are shown in Figures 4.21 and 4.22.

The experiment was started by opening the valves to let the solution flow into the test section at a solution temperature of 80°C. Figure 4.23 shows the results during the first week of the experiment. It can be seen that there was no increase of pressure in the HEP until several hours after start-up. Two days after operating at 80°C, the solution temperature was increased to 300°C.

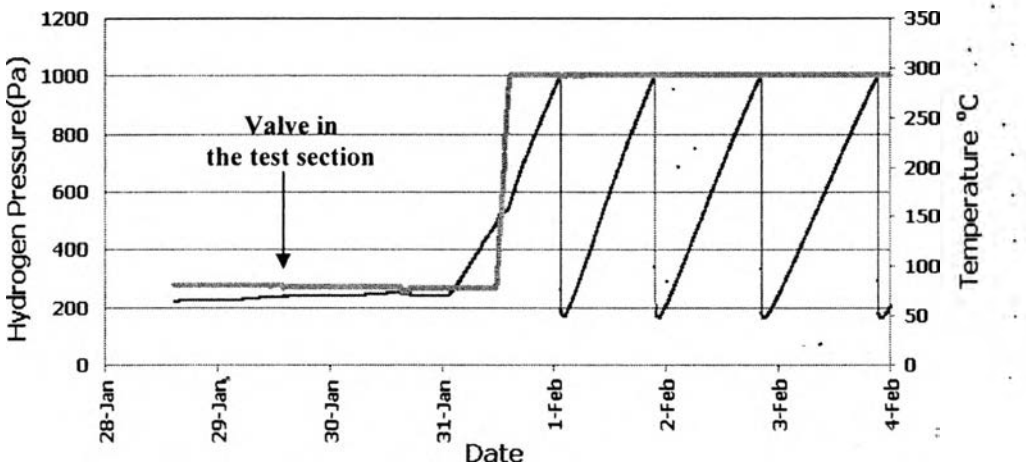

Figure 4.23 The plot of HEP pressure from the experiment on Loop 1 during Oct., 9th and Oct., 15th 2007.

Figures 4.21 and 4.22 showed that the rate of pressure rise and the hydrogen flux were very high after the solution temperature was increased. The rate of pressure rise then gradually decreased until it became constant which is believed indicate a steady state of the corrosion at 300°C. As the solution temperature was decreased from 300°C to 260°C and then to 220°C, the hydrogen flux decreased. The hydrogen flux was high again after the solution temperature increased from 220°C to 300°C.

Then the flux gradually decreased until it was constant. These results show a similar trend to earlier results at this temperature. After operating at 300°C for 15 days, the solution temperature was reduced to 80°C for 2 days before adding oxygen into the solution. At 80°C, the pressure inside the HEP was constant which indicated that there was no hydrogen flux during this period. Several hours after decreasing the solution temperature to 80°C, the pressure started to increase. The rate of pressure rise was constant until the end of this experiment despite a high concentration of oxygen in the solution.

The reason for the delay of the pressure increase may be because there was no oxide film on the metal surface at the beginning of the experiment. Formation of the oxide film is an important factor in making hydrogen diffuse through the metal. Tomlinson (1981, 1989) suggested that the quantity of hydrogen diffusion through the metal depends on the properties and the thickness of the oxide film. The FAC-produced hydrogen tends to go into the solution instead of being absorbed into the metal when the oxide film is not thick enough or has a high porosity. Thus the HEP will not detect hydrogen pressure since the hydrogen will not diffuse through the metal until the oxide film is established although there is FAC and hydrogen is produced as a by-product.

Another possibility is that there was oxygen in the test section prior to starting the experiment i.e. argon contains up to 2 ppm of oxygen and the test section was purged with argon before the test section was valved-in. The presence of oxygen would retard the production of hydrogen by replacing the hydrogen reduction.

A leak of the HEP at the vacuum valve can not be dismissed. It is possible that the corrosion at 80°C is very low. Increases of the pressure at this temperature may be due to the air leakage into the HEP. The leak may become tight as a result of thermal expansion of the metal when the system temperature is increased.

A non-linear increase of the hydrogen pressure was observed in this experiment as shown in Figure 4.24. The pump-down after 1000 Pa was reached was canceled during this period. Thus the highest pressure inside the HEP reached close to 5000 Pa. These results show the same trend as the hydrogen pressure predicted from Fick's Law. However, it is believed that the non-linear hydrogen pressure from

Loop 1 occurred because the corrosion rate had not yet reached steady state. Since the probe used in this experiment was a new bare probe, there was no passive oxide film covering the metal surface initially so the corrosion rate was expected to be high. The corrosion rate decreased as the passive oxide film was produced and covered the metal surface. Thus the non-linearity of the hydrogen pressure rise may be the result of a reduction in corrosion rate.

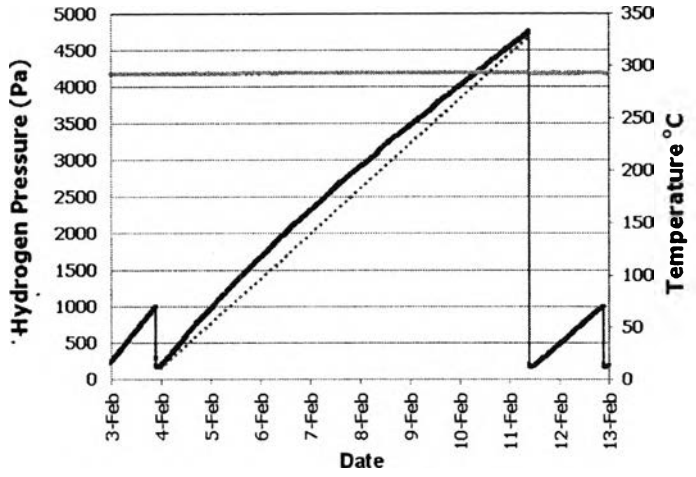

Figure 4.24 The curving of the hydrogen pressure rise from Loop 1.

The effect of temperature was studied in this experiment. The reduction of the pressure rise rate when the solution temperature is reduced indicated that the rate of corrosion decreased as the solution temperature decreased. This behavior agrees with the work of Potter and Mann (1962) which states that the corrosion rate increases with increasing temperature under these conditions due to changes in the solubility of a passive oxide film and changes in the rates of mass transfer. These results imply that the HEP can monitor the change in rate of hydrogen production from corrosion when the process temperature is changed. The results also indicate that the response time of the HEP to the changes in corrosion rate is rapid.

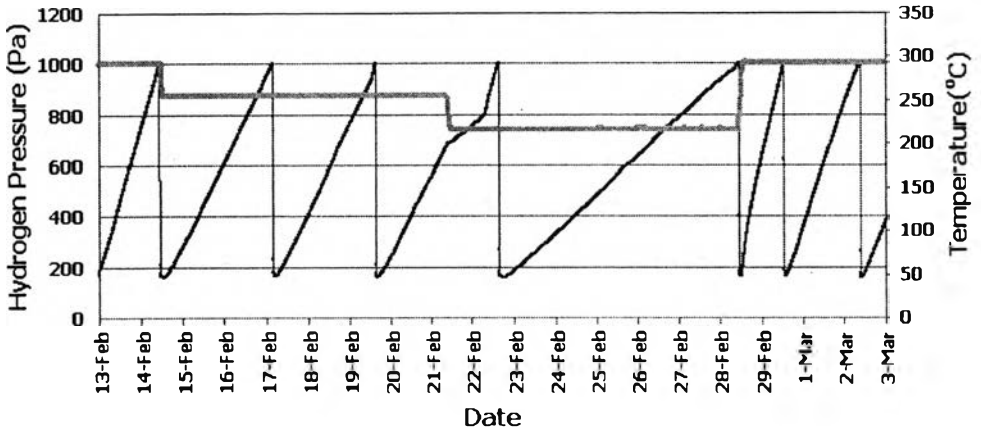

Figure 4.25 The effect of solution temperature on the HEP performance.

On February 22nd, there was an anomaly in the pressure rise rate. After the temperature was reduced from 260 to 220 °C, the rate of pressure rise was reduced for a few hours from the effect of the temperature as shown in Figure 4.25. Then the pressure rise rate increased while the temperature remained constant. It is suspected that the valve connecting the vacuum pump and the pressure transducer was leaking during this period. However, the pressure rise rate decreased again after the HEP pressure was pumped down to full vacuum.

A very high rate of pressure rise is observed after the solution temperature was changed to 300°C which resulted in a high hydrogen flux. Then the rate of pressure rise gradually decreased until a new steady state was reached. When increasing the temperature from 80°C to 300°C, a steady state was reached after 5 days of operation. In the case of increasing the temperature from 220°C to 300°C, a new steady state can be seen after 3 days of operation.

This may be because the oxide film changes its form when the solution temperature changes. It takes a few days for the oxide film to be re-established. Transformation of the oxide film affects both the corrosion rate and the fraction of hydrogen diffusion into the metal; the thinner the oxide film, the higher the corrosion rate and the more hydrogen goes into the solution.

In the case of reducing the temperature from 260°C to 220°C, a new steady state can be seen in a few hours after the temperature decreased. Reducing the temperature from 300°C to 260°C, unintentionally occurred at the same time as a pump-down. However, a new steady state can be seen after a pressure change due to the pump-down. The results indicated that the HEP pressure took a short time to reach a new steady state after the reduction of the temperature. It is expected that a thicker oxide film forms at higher temperatures. Although the thickness of the oxide film decreases as the solution temperature decreases, the corrosion rate is also lower at the lower temperature. Thus the HEP can detect a relatively rapid change of the corrosion rate.

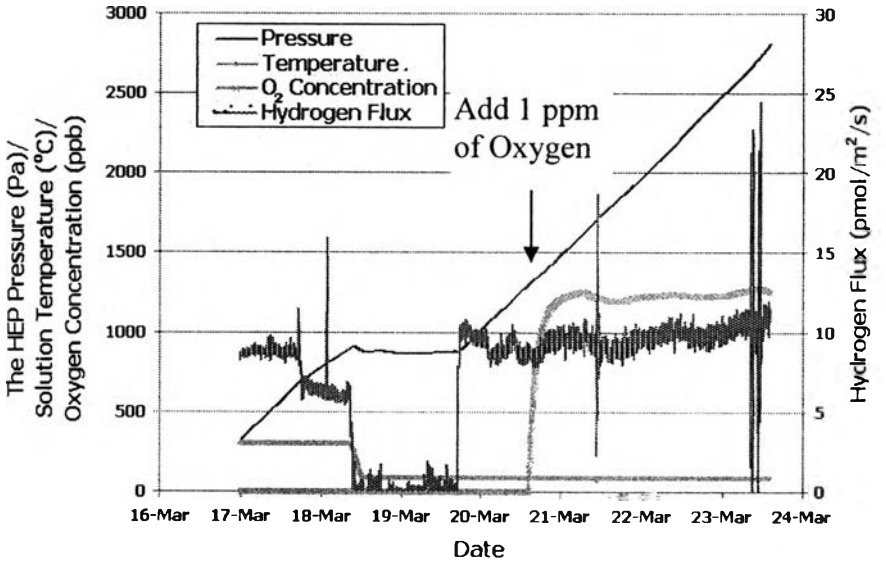

Figure 4.26 The HEP pressure rise during addition of dissolved oxygen into the solution at 80°C.

The presence of dissolved oxygen in the solution is expected to obstruct the hydrogen evolution which leads to a cease of the measured pressure rise from the HEP. In this experiment, however, the pressure continued to increase after oxygen addition with a constant rate of pressure rise as shown in Figure 4.26. Oxygen in the solution seemed to have no effect on the pressure rise.

From the overall plot, it is noticed that the flux was about 10 pmol/m^2/s whenever there was an anomaly in the pressure rise. The time when these anomalies occurred are marked as ① to ④ in Figure 4.21. This phenomenon leads to a query that there might have been air ingress into the HEP which results in a sudden increase of the pressure. If there is any leak in the system, the pressure rise does not represent hydrogen but other gases. It is extremely important to ensure that there is no leak in the HEP.

4.7 Oxygen in the Water Solution

The solution reservoir in the experimental Loop 1 is continuously purged by argon gas in order to maintain a low concentration of oxygen, less than 1 ppb. Nevertheless, a small amount of oxygen gas, i.e. less than 2 ppm, is contained in argon gas. The presence of dissolved oxygen in the solution can affect the corrosion rate and obstruct hydrogen evolution.

The solubility of oxygen is a function of temperature and the partial pressure of oxygen over the water. In this experiment, the reservoir temperature is in the range of 20 to 40°C. The highest dissolved oxygen that could be contained in the solution was considered in this calculation. Due to the fact that the solubility of oxygen is greater in colder water than in warm water, the solution temperature of 20 °C was considered in this calculation.

Oxygen dissolved in water obeys Henry's law. The solubility of oxygen in water is proportional to the partial pressure of oxygen in the air.

$$p_{O_2} = K_{O_2} \cdot x_{O_2} \tag{4.21}$$

where p_{O2} is the partial pressure of oxygen, x_{O2} is the mole fraction of oxygen in oxygen-saturated water, and K_{O2} is the Henry's law constant for oxygen in water.

The Henry's Law constant for oxygen in water is given as a function of temperature as reported by Fernández-Prini *et al.*, (2003) and Watanabe *et al.* (2004).

$$\ln\left(\frac{k_H}{p_1^{\bullet}}\right) = \frac{-9.448}{T_R} + \frac{(4.438)\cdot\tau^{0.355}}{T_R} + 11.420(T_R)^{-0.41}\exp(\tau) \tag{4.22}$$

where $\tau = 1\text{-}T_R$, $T_R = T/T_{Cl}$, T_{Cl} is the critical temperature of the solvent which is 647.096 K for H_2O, and p_1^* is the vapor pressure of the solvent at the temperature of interest.

The results from the calculation show that rate of dissolved oxygen into the solution at 20 °C is 3.94×10^{-11} mol/s (the calculation is shown in Appendix E). The concentration of dissolved oxygen in the solution when purged with argon is 0.09 ppb. In this experiment, the solution flow rate is 840 mL/min or 46.5 mol/min. In this experiment, the solution flow rate is 840 mL/min. Thus the amount of 0.09 ppb of dissolved oxygen in the solution is 2.37×10^{-9} mol/min or 3.94×10^{-11} mol/s.

If oxygen in the system was high prior to valve-in, the oxygen would retard the hydrogen evolution by replacing the reduction reaction of hydrogen ions during FAC. Thus it is recommended that the amount of dissolved oxygen in the solution should be less than 1 ppb. The result from the calculation confirms that the concentration of oxygen is within this specification while the argon is purged into the solution. Furthermore, this small amount of dissolved oxygen is likely consumed by corrosion reactions with the Loop 1 piping prior to reaching the test section.

Nevertheless, there is a possibility that the amount of FAC-produced hydrogen might be consumed by the dissolved oxygen. After starting the process, the oxide film has not yet been established. Oxygen may reach the metal surface and consume the hydrogen before it diffuses into the metal. However, after the oxide film is formed, the oxygen will prevent the hydrogen from being formed by replace the hydrogen reduction. The measured hydrogen flux by the HEP at 80°C is 12×10^{-12} mol/m^2/s. With the permeation area of 3.19 cm^2, rate of hydrogen production is 3.83×10^{-15} mol/s. Thus the oxygen in the solution is several orders of magnitude higher than the rate of hydrogen production. Without the oxide film to retain the hydrogen within the metal/oxide interface, the hydrogen could go into the solution or be consumed by the oxygen. Consequently, the HEP can not detect the hydrogen pressure although there is corrosion at the metal surface.

4.8 The Effect of Capillary Tube Length on the Response Time

A connection between the hydrogen accumulation chamber and the pressure transducer is a capillary tube made of silver. The length of this tubing is several meters in order to reduce the temperature of hydrogen gas before the hydrogen goes into the pressure transducer. O.Yépez *et al.*(1997) studied the effect of the capillary length on the response time of the hydrogen probe. They stated that the hydrogen probe showed a significant delay in the hydrogen pressure response since the molecular hydrogen takes time to transfer from the outside of the pipe throughout the capillary tube and then to be detected by the pressure transducer. A model was developed to explain the time delay caused by the capillary tube.

In their work, it was assumed that the hydrogen transport through the capillary tube was by diffusion through the air. This is obviously not true since there must be no air or very little air inside the capillary tube within a vacuum system. In addition, the velocity of gas transport through a vacuum tube is faster than the speed of sound in the gas since the speed of sound is about 70% of the mean molecular velocity in an ideal gas. Even at room temperature, the speed of sound in hydrogen gas is higher than 1000 m/s (Podesta M.D., 2002). Thus the pressure transducer can instantaneously detect hydrogen that diffuses out from the pipe wall. The effect of the capillary length to the response time is negligible when the pressure inside the HEP is maintained under high vacuum.

This conclusion is supported by the work of Matei (1999) which indicates that the length of the capillary tube and the thickness of the steel specimen have no significant influence on the response time of the hydrogen probe. He stated that the large delay reported in the work of Yépez is caused by the fact that they did not use a proper vacuum pressure or the pressure inside the hydrogen probe was not low enough. Thus the hydrogen probe was insensitive to changes in the hydrogen flux and showed a huge time delay.

It can be concluded that the vacuum within the hydrogen probe should be set low. Thus the response time of the hydrogen probe will be fast due to a negligible time delay. Matei suggested the vacuum should be maintained above -20 kPa compared to atmospheric pressure in the case of the Beta Foil which was used in his

work. For the Hydrogen Effusion Probe (HEP), it has been suggested that the highest pressure inside the HEP should be lower than 2000 Pa. This means whenever the hydrogen pressure inside the HEP reaches 2000 Pa, the vacuum valve will be opened and the hydrogen gas will be pumped out of the HEP by the vacuum pump. Thus the HEP is operated in the absolute pressure range of 0 to 2000 Pa.